

# Development of Starfish-Shaped Two-Ring Microelectromechanical Systems (MEMS) Vibratory Ring Gyroscope with C-Shaped Springs for Higher Sensitivity<sup>†</sup>

Waqas Amin Gill \*, Ian Howard, Ilyas Mazhar and Kristoffer McKee 

Department of Mechanical Engineering, Curtin University, Perth, WA 6845, Australia

\* Correspondence: waqasamin.gill@postgrad.curtin.edu.au

<sup>†</sup> Presented at the 9th International Electronic Conference on Sensors and Applications, 1–15 November 2022;Available online: <https://ecsa-9.sciforum.net/>.

**Abstract:** Microelectromechanical Systems (MEMS) vibratory gyroscopes are one of the integral inertial sensors of the inertial measurement unit (IMU). The usage of MEMS vibratory gyroscopes as inertial sensors has risen enormously in many applications, from household to automotive, smartphones to space applications, smart gadgets to military applications, and so on. This paper presents the mathematical modelling and initial development of the starfish structure with C-shaped springs for a MEMS vibratory ring gyroscope (VRG). The symmetric design methodology of VRGs corroborates higher sensitivity, mode matching, good thermal stability, better resolution, and shock resistance in extreme conditions. The proposed VRG has been designed and investigated using ANSYS<sup>TM</sup> software. This novel design incorporates a two-ring structure, with inner and outer rings, and with 16 C-shaped springs. The outer ring's radius is 1000  $\mu\text{m}$  and the whole VRG structure is supported by the outer eight small square pillars. The gyroscope structure's wine-glass mode driving and sensing resonant frequencies were recorded at 51.50 kHz and 52.16 kHz. The mode mismatch between driving and sensing resonant frequency was measured at 0.66 kHz, which is relatively low compared to the other structures of vibratory gyroscopes. The proposed design provides high shock absorption with higher sensitivity for space applications for the control and manoeuvring of mini satellites for space applications.

**Keywords:** MEMS; starfish; vibratory ring gyroscope; mode matching; space applications; IMU



**Citation:** Gill, W.A.; Howard, I.; Mazhar, I.; McKee, K. Development of Starfish-Shaped Two-Ring Microelectromechanical Systems (MEMS) Vibratory Ring Gyroscope with C-Shaped Springs for Higher Sensitivity. *Eng. Proc.* **2022**, *27*, 36. <https://doi.org/10.3390/ecsa-9-13342>

Academic Editor: Jean-marc Laheurte

Published: 1 November 2022

**Publisher's Note:** MDPI stays neutral with regard to jurisdictional claims in published maps and institutional affiliations.



**Copyright:** © 2022 by the authors. Licensee MDPI, Basel, Switzerland. This article is an open access article distributed under the terms and conditions of the Creative Commons Attribution (CC BY) license (<https://creativecommons.org/licenses/by/4.0/>).

## 1. Introduction

Microelectromechanical system (MEMS) vibratory gyroscopes [1,2] have gained a lot of popularity in the research domain of inertial sensors, and are an integral part of the inertial measurement unit (IMU) [3,4]. The development of MEMS vibrating gyroscopes is thoroughly discussed [5]. The usage of the MEMS gyroscope is quite demanding in many smart devices. MEMS vibratory gyroscopes have been used for a variety of applications in smartphones as inertial sensors. They provide better angular movement detection in digital cameras, transportation of the microscale drug containers in biomedical applications, manoeuvre control and stabilisation of the mini satellites in spacecraft technologies, control and hit the target in missile technology, alongside many other applications [6].

MEMS vibratory ring gyroscopes provide symmetric design, high precision, mode matching and robustness in extreme environments [7], making them ideal candidates for IMU in space applications. Kou et al. developed a new S-shaped spring-based MEMS vibratory ring gyroscope with twenty-four electrodes surrounding the ring structure, both internally and externally [8].

This paper presents the modelling results of a novel design of starfish-shaped MEMS vibratory ring gyroscope for higher sensitivity to harsh environments. The paper discusses

the comparison and advantages of the MEMS vibratory gyroscope of a single-ring to double-ring gyroscope. The concept of adding one more ring increases the overall sensitivity of the gyroscope. The C-shaped spring's symmetric design introduced higher compliance needed for high shock applications. The C-shaped springs absorb a good amount of energy during high-intensity vibrations and support the ring structure.

## 2. Basics of Gyroscopes

The MEMS vibratory gyroscopes operate at two vibrational modes: driving and sensing modes, respectively. In the driving mode, the gyroscope vibrates at a continuous oscillation in the driving axis. The sensing mode detects the gyroscope vibration in the sensing axis when the external rotation is presented.

MEMS vibratory gyroscopes have proof masses “ $m$ ” that operate with two degrees of freedom. In operation, the gyroscope continuously oscillates in one axis direction. There is no oscillation in the other axis direction. However, when the gyroscope experiences an external rotation, the primary oscillation starts shifting on the secondary axis with the Coriolis effect. The two-degree spring-mass system is shown in Figure 1.

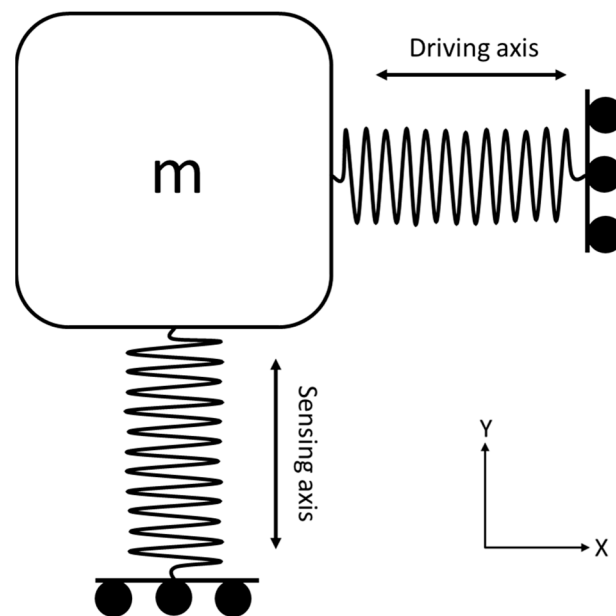


**Figure 1.** A schematic diagram of a simple proof mass of two degrees of freedom.

The basic motion equations of a vibratory gyroscope are written below. Equation (1) gives the motion equation in the driving axis, Equation (2) is about the sensing axis and Equation (3) is the Coriolis force that is produced by the external rotation and the primary oscillation. Here, “ $m$ ” is the proof mass, “ $c$ ” is the damping coefficient, “ $k$ ” is the stiffness constant, “ $x$ ” is the displacement along the driving axis, “ $y$ ” is the displacement along the sensing axis and “ $\Omega$ ” is the external rotation. Here,  $F_D$ ,  $F_S$ , and  $F_C$  are the driving, sensing and Coriolis forces.

$$m\ddot{x} + c\dot{x} + kx = F_D \quad (1)$$

$$m\ddot{y} + c\dot{y} + ky = F_S - F_C \quad (2)$$

$$F_C = -2m\Omega\dot{x} \quad (3)$$

### MEMS Vibratory Ring Gyroscope

MEMS vibratory ring gyroscopes possess many advantages over other gyroscopes, as they have better thermal stability, design symmetry, high precision, high scale factor and better mode matching [9]. The basic design features include a resonator ring, support springs, a centrally placed circular anchor and electrodes for actuation and sensing

purposes [10]. The schematic view of the basic vibratory ring gyroscope is shown in Figure 2.

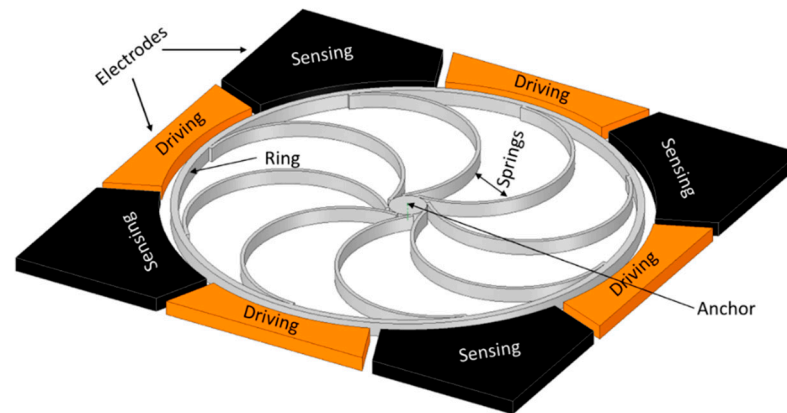


**Figure 2.** A schematic view of vibratory ring gyroscope.

The gyroscope's operating mechanism is described from step 1 to 4 in Figure 3. The ring structure is generally surrounded by eight electrodes related to driving and sensing. The driving electrodes provide a continuous perturbation to the ring structure at the given resonant frequency. The wine-glass mode shape can be seen along the driving electrodes when the device oscillates in the driving axis. Additionally, there is no movement along the sensing electrodes. However, when the gyroscope is subjected to rotation, the wine-glass mode shape transfers towards the sensing electrodes because of the Coriolis force. The change in movement is now sensed by the sensing electrodes.

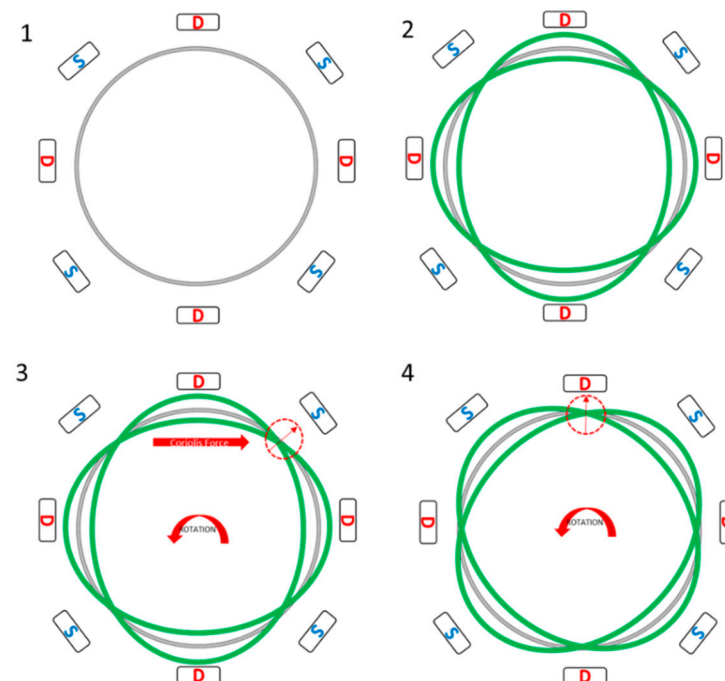


**Figure 3.** Shows operation mechanism of a vibratory ring gyroscope from step 1 to 4.

### 3. Design Methodology of Starfish-Shaped Vibratory Ring Gyroscope

The starfish-shaped gyroscope consists of two resonator rings, sixteen C-shaped springs, and eight small cube shape anchors. There are two sets of C-shaped springs placed in the structure. The outer set has eight springs attached to the outer ring and eight small

anchors. The inner set of springs is attached to the internal and external ring structure. The design features of the proposed gyroscope are listed in Table 1.

**Table 1.** Design features of starfish-shaped MEMS vibratory ring gyroscope.

Design Parameters	Value ( $\mu\text{m}$ )
Outer ring radius	1000
Inner ring radius	650
Ring thickness	15
C spring length	520
C spring arc radius	160
Anchor area	$80 \times 80$

The C-shaped springs are excellent energy-absorbers in the gyroscope structure. The compliance property of the spring is the rate of energy absorption. In harsh environments, especially in high shock or turbulence areas, a gyroscope structure needs to be robust enough to perform with higher sensitivity [11]. The greater compliance of the springs provides better performance in high-shock environments. The proposed C-shaped and starfish structure offers high performance with higher sensitivity and increases the inertial sensor's reliability in harsh environments. The proposed gyroscope design is shown in Figure 4.

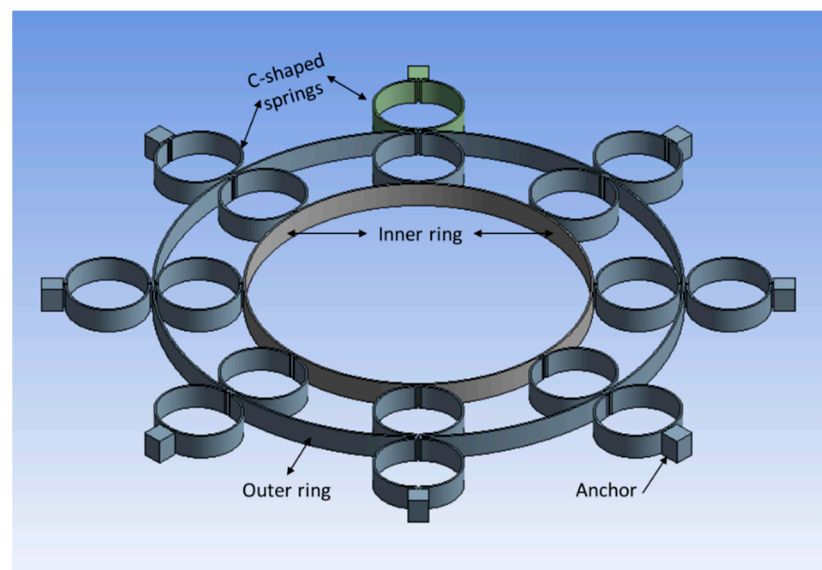


**Figure 4.** The design structure of a starfish-shaped MEMS vibratory ring gyroscope.

The design of the gyroscope will be fabricated with a simple single-wafer silicon-on-insulator (SOI) process. This microfabrication process utilises four masks to pattern the structural layer by deep reactive ion etching (DRIE) process. The structural layer thickness will be  $25\ \mu\text{m}$  and will be suspended on  $400\ \mu\text{m}$  thick substrate.

#### 4. Starfish-Shaped Vibratory Ring Gyroscope Finite Element Analysis

##### 4.1. Modal Analysis

The modal analysis demonstrates the fundamentals of vibrations based on their structures. It gives a detailed analysis of the natural frequency, vibration mode shape and vibration stability. The initial design modelling of the proposed gyroscope was conducted on the ANSYS<sup>TM</sup> software. The vibration modes and the resonant frequencies for modes  $n = 1$  and  $n = 2$  are presented in Figure 5. The wine-glass mode shape can be observed in  $n = 1$  in-plane flexural mode. The triangular circle shape mode can be observed in  $n = 2$

in-plane flexural motion. The  $n = 1$  flexural modes' resonant frequencies for driving and sensing are 51.50 kHz and 52.16 kHz, respectively. The mode mismatch of 0.66 kHz was measured between driving and sensing frequencies.

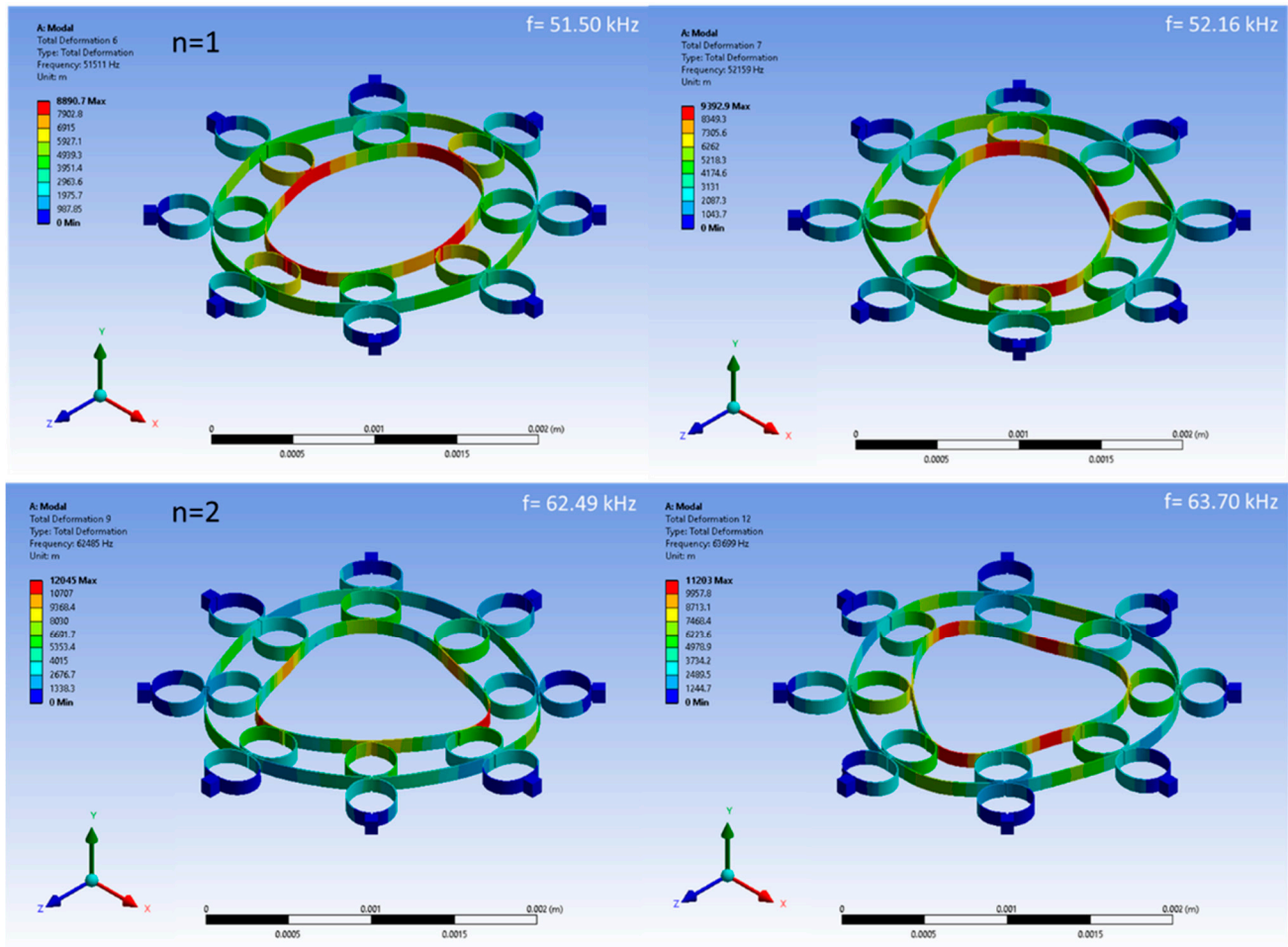


**Figure 5.** Modal frequencies for mode number  $n = 1$  and  $n = 2$ .

#### 4.2. Harmonic Analysis

To determine the displacement response of the gyroscope resonator structure up on electrostatic force is quite important. A harmonic analysis study was performed on the ANSYS<sup>TM</sup> software to obtain the frequency-amplitude response when a certain perturbation force is applied to the structure. The two peak values were observed for driving and sensing frequencies, respectively.

In the directions of  $0^\circ$  and  $180^\circ$ , a  $1 \mu\text{N}$  force of simple harmonic was applied to the ring structure in the driving direction. The amplitude response after applying harmonic force is shown in Figure 6. A resonant peak can be seen at 51.50 kHz frequency, with a vibration amplitude of  $0.17 \mu\text{m}$  in the driving direction.

A harmonic response in the sensing direction was investigated by providing an actuation force of  $1 \mu\text{N}$  in the sensing directions of  $45^\circ$  and  $225^\circ$ . The resonant peak at 52.16 kHz frequency with an amplitude response of  $0.019 \mu\text{m}$  in the sensing direction is observed in Figure 6.

There are two MEMS vibrating ring gyroscope designs compared in Table 2, alongside the proposed vibrating ring gyroscope. The initial result of mode mismatch is quite high. However, the mode mismatch issue will be resolved with parametric analysis of the design parameters.

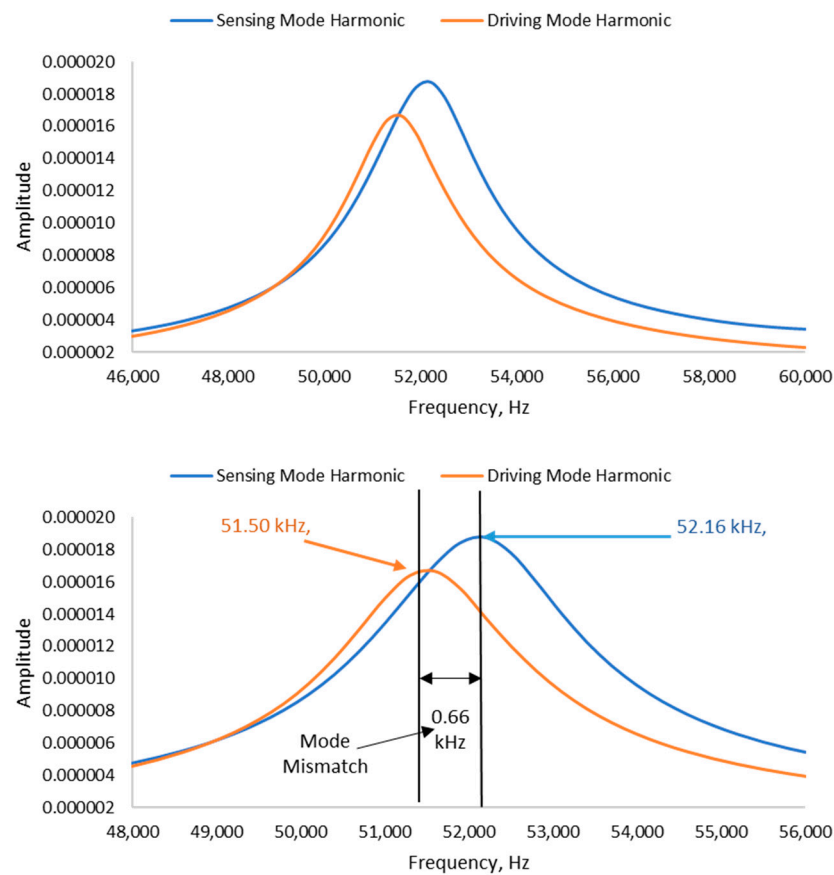


**Figure 6.** A harmonic response for the amplitude-frequency response.

**Table 2.** Comparison with similar vibrating ring gyroscope designs.

References	Institution	Design	Ring Radius, $\mu\text{m}$	Driving Frequency, kHz	Sensing Frequency, kHz	Mode Mismatch, Hz
	Curtin University, Australia	Starfish shaped, two rings	1000	51.50	52.16	660
[7]	North University of China, China	Double U-Beam vibrating ring	1500	9.61	9.62	16
[10]	Khalifa University of Science and Technology, UAE	(100) Silicon vibrating ring	750	21.443	21.438	5

## 5. Conclusions

We have successfully developed a starfish-shaped MEMS vibratory ring gyroscope with high robustness for higher sensitivity. The two ring resonators and the inclusion of sixteen C-shaped springs corroborate higher compliance for high-shock environments. The 160  $\mu\text{m}$  arc radius and 520  $\mu\text{m}$  length of the C springs are best to absorb energy in high-shock vibrations, and their symmetric design also provides good thermal stability. The vibratory ring gyroscope with a ring radius of 1000  $\mu\text{m}$  has wine-glass mode frequencies at 51.50 kHz for driving and 52.16 kHz for sensing. The mode mismatch of 0.66 kHz is measured between driving and sensing resonant frequencies. The harmonic amplitude response for driving is 0.017  $\mu\text{m}$ , while for sensing, it is 0.019  $\mu\text{m}$ . The starfish-shaped MEMS vibratory gyroscope's symmetric design methodology initially provided excellent results for vibratory gyroscopes with higher sensitivity in harsh environments.



**Author Contributions:** The conceptualisation and idea were provided by W.A.G. The design, findings and preparation of the figures were conducted by W.A.G. Writing: the draft was written by W.A.G. Writing: review and editing of the final draft was completed by I.H., I.M. and K.M. All authors have read and agreed to the published version of the manuscript.

**Funding:** This research received no external funding.

**Institutional Review Board Statement:** Not applicable.

**Informed Consent Statement:** Not applicable.

**Data Availability Statement:** Not applicable.

**Conflicts of Interest:** The authors declare no conflict of interest.

## References

1. Passaro, V.M.N.; Cuccovillo, A.; Vaiani, L.; De Carlo, M.; Campanella, C.E. Gyroscope Technology and Applications: A Review in the Industrial Perspective. *Sensors* **2017**, *17*, 2284. [[CrossRef](#)] [[PubMed](#)]
2. Xia, D.; Yu, C.; Kong, L. The Development of Micromachined Gyroscope Structure and Circuitry Technology. *Sensors* **2014**, *14*, 1394–1473. [[CrossRef](#)] [[PubMed](#)]
3. Mohammed, Z.; Gill, W.; Rasras, M. Modelling optimization and characterization of inertial sensors. In *Nanoscale Semicon-Ductor Devices, MEMS, and Sensors: Outlook and Challenges*; Springer: Berlin/Heidelberg, Germany, 2017.
4. Mohammed, Z.; Gill, W.A.; Rasras, M.J.I.S.L. Double-comb-finger design to eliminate cross-axis sensitivity in a dual-axis accelerometer. *IEEE Sens. Lett.* **2017**, *1*, 2501004. [[CrossRef](#)]
5. Gill, W.A.; Howard, I.; Mazhar, I.; McKee, K. A Review of MEMS Vibrating Gyroscopes and Their Reliability Issues in Harsh Environments. *Sensors* **2022**, *22*, 7405. [[CrossRef](#)] [[PubMed](#)]
6. Lee, J.S.; An, B.H.; Mansouri, M.; Al Yassi, H.; Taha, I.; Gill, W.A.; Choi, D.S. MEMS vibrating wheel on gimbal gyroscope with high scale factor. *Microsyst. Technol.* **2019**, *25*, 4645–4650. [[CrossRef](#)]
7. Cao, H.; Liu, Y.; Kou, Z.; Zhang, Y.; Shao, X.; Gao, J.; Huang, K.; Shi, Y.; Tang, J.; Shen, C.; et al. Design, Fabrication and Ex-periment of Double U-Beam MEMS Vibration Ring Gyroscope. *Micromachines* **2019**, *10*, 186. [[CrossRef](#)] [[PubMed](#)]
8. Kou, Z.; Liu, J.; Cao, H.; Shi, Y.; Ren, J.; Zhang, Y. A novel MEMS S-springs vibrating ring gyroscope with atmosphere package. *AIP Adv.* **2017**, *7*, 125301. [[CrossRef](#)]
9. Syed, W.U.; An, B.H.; Gill, W.A.; Saeed, N.; Al-Shaibah, M.S.; Al Dahmani, S.; Choi, D.S.; Elfadel, I.A.M. Sensor Design Mi-gration: The Case of a VRG. *IEEE Sens. J.* **2019**, *19*, 10336–10346. [[CrossRef](#)]
10. Hyun An, B.; Gill, W.A.; Lee, J.S.; Han, S.; Chang, H.K.; Chatterjee, A.N.; Choi, D.S. Micro-electromechanical vibrating ring gyroscope with structural mode-matching in (100) silicon. *Sens Lett.* **2018**, *16*, 548–551.
11. Gill, W.A.; Ali, D.; An, B.H.; Syed, W.U.; Saeed, N.; Al-Shaibah, M.; Elfadel, I.M.; Al Dahmani, S.; Choi, D.S. MEMS mul-ti-vibrating ring gyroscope for space applications. *Microsyst. Technol.* **2020**, *26*, 2527–2533. [[CrossRef](#)]